NASA TN D-1332

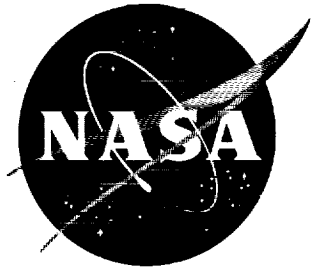

TECHNICAL NOTE

D-1332

MEASUREMENTS OF THE EFFECTIVE HEATS OF ABLATION OF TEFLON AND POLYETHYLENE AT CONVECTIVE HEATING RATES FROM 25 TO 420 BTU/FT^2 SEC

By Dale L. Compton, Warren Winovich, and
Roy M. Wakefield

Ames Research Center
Moffett Field, Calif.

NATIONAL AERONAUTICS AND SPACE ADMINISTRATION
WASHINGTON

August 1962

NATIONAL AERONAUTICS AND SPACE ADMINISTRATION

TECHNICAL NOTE D-1332

MEASUREMENTS OF THE EFFECTIVE HEATS OF ABLATION OF TEFLON AND POLYETHYLENE AT CONVECTIVE HEATING RATES FROM 25 TO 420 BTU/FT^2 SEC

By Dale L. Compton, Warren Winovich, and
Roy M. Wakefield

SUMMARY

Experiments were conducted in an air arc wind tunnel to determine the effective heats of ablation of teflon at convective heating rates of 25 to 80 Btu/ft^2 sec, and of polyethylene at convective heating rates of 25 to 417 Btu/ft^2 sec. The nominal total enthalpy of the tests was 2,500 Btu/lb. A comparison of the data thus obtained with data from previous tests at higher heating rates shows that the effective heat of ablation of teflon is independent of heating rate in the range from 25 to 21,000 Btu/ft^2 sec, and that the effective heat of ablation of polyethylene at 25 to 420 Btu/ft^2 sec is reduced to approximately 50 to 75 percent of its value at 15,000 to 21,000 Btu/ft^2 sec. The explanation of these results is that teflon ablates by subliming, whereas polyethylene ablates with both molten material and vapor as products. The proportion of melt flow to vapor flow for polyethylene was found to vary with heating rate, becoming smaller as the heating rate was increased.

Computations to determine the depths of penetration of the maximum temperatures for which the two ablation materials tested are structurally useful show that severe penetrations occur for the case of steady-state ablation at low heating rates.

INTRODUCTION

In most reentry heating research to date, emphasis has been placed on solving the heat-shield problem for the blunt front surfaces of spacecraft entering the atmosphere on relatively steep trajectories, characterized by high heating rates for short periods of time. Ablation heat-shield materials have been found that perform well in this environment which minimizes the diffusion of heat into the heat shield. The question arises as to whether these materials will also perform satisfactorily for the relatively low, long-duration heating rates that will occur on the afterbodies of spacecraft entering on shallow trajectories. If the heating rate is sufficiently low, it is conceivable that the surface of the ablation heat shield may not be brought up to ablation temperature before

much of the heat has diffused through the heat shield. Thus, as a minimum, the effectiveness of the heat shield would be reduced and it is possible that the heat shield may melt away or slump off before it has performed as an ablator.

It was the purpose of the study reported herein, therefore, to determine the effective heat of ablation at low heating rates for two ablators - one which sublimes, teflon, and one which normally melts and vaporizes, polyethylene. The heating rates were 25 to 80 Btu/ft^2 sec for teflon and 25 to 417 Btu/ft^2 sec for polyethylene. The stagnation enthalpy was nominally 2,500 Btu/lb.

A second purpose was to consider briefly the possibility of a catastrophic failure of a thermoplastic heat shield by slumping or melting. Calculations are presented to show the depths of penetration of the maximum temperatures for structural usefulness into polyethylene and teflon for various conditions of heating rate and total enthalpy.

SYMBOLS

A	area, ft^2
c	specific heat, Btu/lb $^\circ$R
d	diameter, ft
h	enthalpy, Btu/lb
h_{eff}	effective heat of ablation, Btu/lb
k	coefficient of thermal conductivity, Btu/sec ft $^\circ$R
m	mass, lb
$\dot{m}$	mass loss rate per unit area, lb/ft^2 sec
$\dot{m}_m$	$\frac{\text{mass loss per unit area}}{\text{run duration}}$, $\frac{\text{lb}}{\text{ft}^2\text{sec}}$
M	Mach number, dimensionless
p	pressure, atm
$\dot{q}$	heat-transfer rate, Btu/ft^2 sec
R	nose radius, ft
t	time, sec

t_a time at which the ablation surface reaches the ablation temperature, sec

T temperature, ^{o}R

V velocity, ft/sec

w air mass flow rate, lb/sec

x distance from the ablation surface into the material, ft

α thermal diffusivity, ft^2/sec

β transpiration parameter, dimensionless

γ isentropic exponent, dimensionless

Γ vapor ratio, $\frac{\dot{m}_v}{\dot{m}}$, dimensionless

Δm mass loss, lb

ρ density, lb/ft^3

Subscripts

a ablation

l liquid

ms maximum service

o initial conditions in the ablation material

r reservoir

t total

v vapor

w wall

cl center line

2 conditions behind a normal shock

Superscript

* conditions at the nozzle throat

EXPERIMENT

Facility

Description.- Tests were conducted in the arc-jet facility shown schematically in figure 1. Air introduced into the lower end of the air chamber is heated by a direct-current arc between the concentric ring-shaped electrodes, is expanded through the nozzle at the top of the chamber, passes over the test model, and is exhausted to a large vacuum sphere. To prevent melting of the electrodes and to reduce air-stream contamination the copper electrodes are water cooled, and the arc is rotated around the electrode rings at about 1,000 cycles per second by a magnetic field established at right angles to the arc column. The electrodes and magnetic pole pieces are enclosed in a pressure-tight steel shell allowing the unit to be operated at preselected stagnation pressures. The nozzle is stainless steel with a copper entrance section and is attached to the upper pole piece. The spacing between the electrodes and nozzle entrance insures a sufficient residence time for the air after it has been heated so that all species are in equilibrium when the air leaves the heater. The shell, magnetic pole pieces, and nozzle are uncooled and, hence, limit the running time of the unit.

Nozzle sizes and nominal conditions for the present test are given below.

Stagnation-point heat-transfer rate, Btu/ft^2 sec	25-130	278	417
Stagnation enthalpy (nominal), Btu/lb	2500	2500	2500
Nozzle throat diameter, in.	0.75	0.75	0.75
Nozzle exit diameter, in.	2.68	2.68	1.25
Mach number	3.8	3.8	2.2
Total reservoir pressure, atm	0.25	0.50	1.70
Nozzle exit stagnation pressure, atm	0.031	0.062	0.75

Stagnation enthalpy measurements.- The stagnation enthalpy was determined by the equilibrium sonic flow method. This method is based upon the fact that for a real gas at a given stagnation pressure the parameter, ρ^*V^*/p_{t_r}, is a unique function of the stagnation enthalpy. For the reversible, adiabatic, one-dimensional flow of a perfect gas, this relation can be derived in closed form and, for $\gamma = 1.4$, is given by

$$\frac{\rho^*V^*}{p_{t_r}} = \frac{w}{p_{t_r}A^*} = 552\ h_t^{-1/2} \qquad (1)$$

For the flow of a real gas, ρ^*V^*/p_{t_r} must be evaluated numerically as shown in figure 2. The equation of state for air was taken from the charts of reference 1. Thus metering air-flow rate, measuring total reservoir pressure, and knowing the nozzle throat area made it possible to determine the value of the stagnation enthalpy.

The nominal stagnation enthalpy for the tests was 2,500 Btu/lb. However, variations in the operation of the arc unit resulted in actual test enthalpies in the range from 2,000 to 3,000 Btu/lb.

Pressure surveys in test region.- It was deemed desirable to obtain information on the uniformity of the supersonic air stream. The Mach number 3.8 nozzle was chosen for air-stream calibration for the following reasons: (1) Models of different diameters were tested in this nozzle, whereas only one model size was tested in the Mach number 2.2 nozzle; (2) the lowest reservoir pressures and, hence, the lowest Reynolds numbers were encountered in the $M = 3.8$ nozzle; and (3) the largest ratio of model diameter to nozzle exit diameter occurred for this nozzle. Accordingly, a total pressure survey of the air stream at the nozzle exit was conducted for a total reservoir pressure of 0.25 atmosphere. The results are presented in figure 3. It can be seen from this figure that the total pressure was reasonably constant over a 1-inch-diameter core around the nozzle center line. Beyond this diameter, the total pressure rose rapidly, then dropped sharply near the edge of the free jet. As will be explained later, all the models, with one exception, had maximum diameters within the 1-inch-diameter core flow.

A Mach number distribution at the nozzle exit plane was computed from measurements of total reservoir pressure, stagnation pressure behind a normal shock, and static pressure on the wall at the nozzle exit. For this computation the static pressure was assumed to have its wall value at all points in the nozzle exit plane and the stagnation enthalpy was assumed constant across the stream. The results of this computation are shown in figure 4.

Ablation and Heating Rate Measurements

A useful ablation parameter is the effective heat of ablation, h_{eff}, defined as

$$h_{eff} = \frac{\dot{q}}{\dot{m}} \tag{2}$$

where $\dot{m}$ is the mass-loss rate per unit area from the ablating surface, and $\dot{q}$ is the heat-transfer rate to the surface (in the absence of ablation) at the surface temperature at which ablation occurs. To determine h_{eff} experimentally, it is necessary to measure both the mass-loss rate and the heating rate. The following sections describe the models and techniques used for these measurements.

Ablation models and test conditions.- Stagnation-region ablation rate measurements were made on polytetrafluorethylene (teflon) and linear high-density polyethylene (specific gravity = 0.953). A sketch of the model shape used for tests at heating rates below 100 Btu/ft^2 sec is shown in figure 5. Model diameters were 1.5, 0.75, 0.50, and 0.25 inch with corresponding radii of curvature in the stagnation region of twice the diameter. This shape was chosen to give a low value of the stagnation point heating rate for a given diameter. A sketch of the model used for the heating rate tests above 100 Btu/ft^2 sec is shown in figure 6. This model had a diameter of 0.50 inch and a radius of curvature in the stagnation region of 0.375 inch. This shape was chosen to give negligible shape change for the larger ablation recession distances associated with the higher heating rate tests of polyethylene.

To avoid corner effects and to maintain a nearly constant heating rate over the part of the model being tested, the models were machined in two pieces - an insert pressfitted into a concentric shroud. The variation in heat-transfer rate across the face of the insert was less than 3 percent of the stagnation value for the models used in the low heating rate tests and less than 10 percent for the models used in the higher heating rate tests, as shown by the analysis and measurements of reference 2. In addition, this model construction method permitted mass-loss measurements to be made directly in the stagnation region. The table below gives the test conditions for each heating rate.

Ablation material	$\dot{q}$, Btu/ft^2 sec	Model diameter, in.	Nozzle Mach no.	Total reservoir pressure, atm	Total enthalpy, Btu/lb
Teflon	21.6	1.50	3.8	0.25	2190
↓	44.7	.75	↓	↓	2490
	61.2	.50			2700
	87.0	.25			2990
Polyethylene	24.0	1.50	3.8	0.25	2280
↓	40.3	.75	↓	↓	2320
	45.7	.50			2170
	65.6	.25			2200
	105	.50		↓	2000
	278	.50	↓	.50	2800
	417	.50	2.2	1.7	2250

The 1.5-inch-diameter model was the only model which extended beyond the region of substantially uniform flow in the M = 3.8 nozzle; however, the 0.75-inch-diameter insert on this model was well within the uniform region.

Test procedure.- Before being tested, each insert was weighed on a precision balance to determine its mass to the nearest 0.1 milligram. For the ablation test the model was then placed on the nozzle center line 1 inch from the nozzle exit plane, the free-jet chamber was evacuated, the air flow was started, and the arc was run for the desired length of time. After completion of the run, the model was removed from the tunnel and the insert reweighed to determine the mass loss. Typical photographs of models undergoing ablation are shown in figure 7. The dark area on the side of the polyethylene model in figure 7(b) is an accumulation of resolidified material which flowed from the front face.

In order to determine whether the radius of curvature of the insert and, consequently, the stagnation heat-transfer rate had changed during a test, contour photographs of each test model were taken after testing and compared with the contour before testing. These photographs showed that the stagnation region radius of curvature remained nearly constant during the tests. Typical photographs of this type are shown in figure 8(a) for the 0.75-inch-diameter teflon models and in figure 8(b) for the 0.75-inch-diameter polyethylene models. The white line shows the original shape, while the darkened area shows the final shape. The material in figure 8(b) that extends beyond the original model shape is polyethylene, which ablated as a liquid and then solidified on the model afterbody.

An examination of the teflon models after testing showed a slight gap on the front surface at the interface between the shroud and insert. The width of this gap (0.02 inch) was found to be independent of model diameter and run duration. For the polyethylene models, the flow of liquid on the ablating surface welded the insert to the shroud.

Determination of steady-state mass-loss rate.- In order to obtain the steady-state mass-loss rate from the mass-loss data, it was necessary to take account of the transient phenomena. Briefly stated, there are three transient periods: (1) The time required for the arc and flow to be established; (2) the time required for the surface of the model to come to the ablation temperature; and (3) the time required for steady-state ablation to be established. The length of time for transient (1) was approximately 0.1 second as determined from measured pressure transients - considered negligible when compared to the total run duration. The lengths of time for transients (2) and (3) depend on the properties of the ablation material, the stagnation enthalpy, and the heat-transfer rate and may be of the order of several seconds (ref. 3). The corrections to obtain steady-state mass-loss rates from the mass-loss data were determined experimentally and are described below.

Steady-state ablation rates for the models run at heating rates of 25 to 40 Btu/ft^2 sec (the 1.5- and 0.75-inch-diameter models) were obtained by running several models of each diameter for different durations of time - nominally, 5, 10, 15, and 20 seconds. The mass loss per unit area was then plotted as a function of run duration and from this plot the steady-state mass-loss rate was determined from measurements of the

final slope of the curve. These plots are shown in figure 9(a) for teflon and in figure 9(b) for polyethylene. It can be seen that in some cases appreciable error in the mass-loss rate would result from simply dividing the mass loss by the total run duration.

The same procedure was used for the heating rate tests at 105, 278, and 417 Btu/ft^2 sec, except that running times were 2, 4, 6, 8, and 10 seconds.

Steady-state mass-loss rates for the models tested at heating rates of 61 and 80 Btu/ft^2 sec for teflon and 46 and 66 Btu/ft^2 sec for polyethylene were obtained from only one duration of run for each model by the following method. It is shown in reference 3 that, for a given ablation material and total enthalpy, the durations of transients (2) and (3) are decreasing functions of the heating rate, $\dot{q}$. Consider the ratio $\dot{m}_m/\dot{m}$, where $\dot{m}_m$ is the measured mass loss per unit area divided by the total running time, and $\dot{m}$ is the steady-state mass-loss rate. For a given run duration, this ratio depends on the transient times and therefore is a function of the heating rate. Physically, this ratio represents the amount by which the actual mass loss from any run would need to be corrected to obtain the steady-state mass loss. From the measured values of $\dot{m}_m/\dot{m}$ for the models tested near heating rates of 25 and 40 Btu/ft^2 sec, the corrections for the other two models were obtained by plotting $\dot{m}_m/\dot{m}$ versus $1/\dot{q}$ and reading the values of $\dot{m}_m/\dot{m}$ at the higher heating rates. These corrections were then applied to the actual mass loss to obtain the steady-state mass loss. The magnitudes of these corrections were small, amounting to only a few percent.

Heat-transfer models.- Heat-transfer-rate measurements were made on three nonablating models with maximum diameters of 1.5, 0.75, and 0.50 inch, and with corresponding radii of curvature in the stagnation region of 3.0, 1.5, and 0.375 inch, respectively. A sketch of the 0.75-inch-diameter model is shown in figure 10. (The 1.5-inch and 0.50-inch-diameter models differed from this only in size and minor detail.) The models were machined with a stainless steel outer shell and a copper calorimeter of the same diameter as that of the insert on the corresponding ablation model. The calorimeter was set flush with the front face of the shell and supported by small pins. It was held in place on bakelite pins protruding from a retaining plug. Computations showed that this support system resulted in negligible conduction losses from the calorimeter. The calorimeter was instrumented with a chromel-alumel thermocouple placed approximately in its center. The thermocouple leads were shielded to avoid electrical interference from the arc, and the output was recorded on an oscillograph to obtain the time history of the calorimeter temperature.

Determination of heating rate.- The heat-transfer rate was calculated from the relation

$$\dot{q} = \frac{mc}{A}\frac{dT}{dt} \qquad (3)$$

where m and A are the mass and front surface area of the calorimeter, c, its specific heat, and dT/dt the measured slope of the temperature versus time curve. The relative error of the heat-transfer measurements was about ±5 percent.

Since the calorimeters had finite thicknesses, computations were performed to determine whether the time derivative of temperature at the thermocouple location (near the center of the calorimeter) was a good representation of the time derivative of temperature near the front surface. These computations showed that for times greater than 0.1 second the slope at the thermocouple location differed by less than 1 percent from the slope at the front surface.

The heat-transfer rates measured were compared with those computed from the theory of reference 4. Heat-transfer results are compared in figure 11. The agreement between theory and experiment was within 15 percent.

To obtain the heat-transfer rate to the ablating models in the absence of ablation, a correction was applied to the calorimeter heat-transfer rates to account for the difference in surface temperature between the calorimeter surface and the ablation surface. Surface temperatures were taken to be 1,400° F for teflon and 1,000° F for polyethylene.

RESULTS AND DISCUSSION

Experimental Results

From the measured heat-transfer rates and mass-loss rates the effective heats of ablation for polyethylene and teflon were calculated from equation (2). The effective heats of ablation are plotted as a function of heating rate in figure 12(a) for teflon and in figure 12(b) for polyethylene. Some of the apparent scatter in the measured values of h_{eff} may be due to the slight differences in test enthalpy level. Included in figure 12(a) are the values of h_{eff} obtained in the tests of references 5 and 6, at heating rates of 250 to 380 and 15,000 to 21,000 Btu/ft^2 sec, respectively, and at an enthalpy potential of 2,500 Btu/lb. From the good agreement of the present data with the higher heating rate data, it can reasonably be concluded that the effective heat of ablation of teflon is not a function of heating rate in the range from 25 to 21,000 Btu/ft^2 sec. As shown in figure 12(b) the value of h_{eff} for polyethylene from the 15,000 to 21,000 Btu/ft^2 sec heating-rate tests of reference 6 is approximately 1-1/2 to 2 times that measured in the present tests. This difference is probably attributable to the fact that for the present tests the fraction of material lost as liquid is higher than in the tests of reference 6.

It is of interest to consider this point in more detail. The theory of reference 7 can be used to write the effective heat of ablation (in the nomenclature of the present report) as

$$h_{eff} = \Gamma\left[(h_w - h_o) + \beta(h_t - h_w)\right] + (1 - \Gamma)(h_l - h_o) \qquad (4)$$

where Γ is the ratio of mass-loss rate by vapor to total mass-loss rate

$$\Gamma = \frac{\dot{m}_v}{\dot{m}} \qquad (5)$$

Thus for given free-stream conditions and a given ablative material, h_{eff} is a linear function of Γ, taking on its maximum value when $\Gamma = 1.0$ corresponding to the case where all of the ablated material is vaporized at the surface. The value of Γ will depend on the material, the heating rate, the deceleration to which the vehicle is subjected, and the flight conditions. High heating rates, high material viscosities, and high decelerations will promote high values of Γ.

In order to determine quantitatively the influence of heating rate on h_{eff} through its influence on Γ, a series of calculations for polyethylene was made on an IBM 7090 computer. These calculations gave solutions for the two-phase, liquid-gas boundary layer for the conditions of the present tests and the tests of reference 6. The details of this unpublished solution were developed by Dr. Dean R. Chapman of the Ames Research Center. Since the properties of liquid polyethylene are not well known, the solutions were obtained by matching the theory to the data at a heating rate of 40 Btu/ft^2 sec and then allowing the theory to predict the variation of h_{eff} with heating rate over the heating-rate range from 20 to 20,000 Btu/ft^2 sec. The results of these calculations are shown as a curve in figure 12(b). It can be seen that the trend of the curve agrees reasonably well with the present data.

A value of $\Gamma = 0.6$ for polyethylene has been determined experimentally in nitrogen (ref. 8) for conditions of heating rate and enthalpy near the low heating-rate conditions in the present report. A value of $\Gamma = 0.5$ is obtained for the present tests at heating rates less than 100 Btu/ft^2 sec, if $\Gamma = 1$ is assumed for the tests of reference 6. This correlation between the experimental value of Γ from reference 8 and the value of Γ calculated from the experimental results of the present paper is a further indication that the measured reduction in h_{eff} at low heating rates is due primarily to liquid ablation.

From the above comparisons, it may be reasonably concluded that for subliming ablators such as teflon, low heating rates will not change h_{eff}, while for melting and vaporizing ablators such as polyethylene, low heating rates will adversely affect h_{eff}, by increasing the runoff of molten material.

Effect of Low Heating Rate on Temperature Penetration

Another effect of low heating rates on ablation materials will be to cause an increase in thermal thickness by altering the temperature distribution within the ablating material. If a step heat impulse of constant value is assumed (approximately the conditions for the present tests), it is possible to compute the length of time, t_a, required for the surface of the material to come to the ablation temperature, T_a, and the temperature distribution within the material at the time ablation begins. The appropriate equations for a one-dimensional, semi-infinite slab are (ref. 9)

$$t_a = \frac{\pi k^2 (T_a - T_o)^2}{4\dot{q}^2 \alpha} \tag{6}$$

and

$$(T - T_o) = (T_a - T_o) \sqrt{\pi}\ \text{ierfc}\ \frac{x}{2\sqrt{\alpha t_a}} \tag{7}$$

The value of t_a could also be determined experimentally from motion picture studies of the ablating models by observing the time at which ablation products first appear in the boundary layer. The values of t_a from equation (6) and from experiment are plotted as a function of heating rate in figure 13. The agreement is reasonably good for the teflon models but is poor for the polyethylene models. The reason for the poor agreement of the polyethylene data is not known, but may be due to the fact that some vaporization of polyethylene may begin at a lower surface temperature than the steady-state ablation temperature, or that the assumption of 1000° F as an ablation temperature for polyethylene is too high. If the ablation temperature were assumed to be 700° F, then the agreement would have been excellent.

For these materials a temperature may be defined above which the material no longer has sufficient strength to be of use structurally. For teflon this temperature is 500° F (ref. 10), and for polyethylene 250° F (the experimentally determined melting temperature). These temperatures will be designated as maximum service temperatures and denoted by T_{ms}. The depths of penetration, x_{ms}, of T_{ms} were calculated from equation (7) and the theoretical values for t_a. The values of x_{ms} are plotted as a function of heating rate in figure 14. It can be seen that, except for very low heating rates, the depths of penetration of the maximum service temperatures at the time ablation begins are not severe.

The depths of penetration of the maximum service temperatures may also be computed for conditions of steady-state ablation. The appropriate

equation (in the present nomenclature) is (ref. 3)

$$x_{ms} = \frac{\rho\alpha\, h_{eff}}{\dot{q}} \ln \frac{T_a - T_o}{T_{ms} - T_o} \tag{8}$$

Thus, for the steady-state ablation case, x_{ms} depends on the value of h_{eff} as well as on the heating rate, increasing with decreasing heating rate and with increasing h_{eff}. Values of x_{ms} for teflon and polyethylene were calculated as functions of heating rate for the following two cases: (1) The value of h_{eff} was taken as 1,500 Btu/lb, approximately the value from the present tests, and (2) values of h_{eff} were assumed which might apply to these materials at escape velocity. These values were obtained by extrapolating the results of reference 6. The values of x_{ms} thus calculated are plotted as a function of heating rate in figure 15. This figure shows that the depths of penetration of the maximum service temperatures under some conditions of steady-state ablation can be quite severe, particularly for low heating rates at high velocities.

CONCLUSIONS

Experimental measurements of the effective heats of ablation of teflon and polyethylene have been made in an air arc wind tunnel at heating rates from 25 to 420 Btu/ft^2 sec and at a nominal stagnation enthalpy of 2,500 Btu/lb. The following conclusions were reached:

1. Comparison of the experimental results with data taken at higher heating rates shows that the effective heat of ablation of teflon is independent of heating rate over the range of heating rates from 25 to 20,000 Btu/ft^2 sec.

2. Comparison of the experimental data for polyethylene with higher heating rate results shows that the effective heat of ablation of polyethylene at 25 to 420 Btu/ft^2 sec is reduced to approximately 50 to 75 percent of the value that has been reported for a heating-rate range of 15,000 to 21,000 Btu/ft^2 sec. Calculations show that this reduction in h_{eff} for polyethylene is due to loss of ablated material in the molten state. Solutions of the appropriate two-phase boundary-layer equations show fair agreement with the trend of the experimental polyethylene data.

3. Computations to determine the depths of penetration of the maximum service temperatures into teflon and polyethylene show that severe penetration occurs under conditions of steady-state ablation. This constitutes a serious problem for low heating rates and high velocities.

Ames Research Center
National Aeronautics and Space Administration
Moffett Field, Calif., April 16, 1962

REFERENCES

1. Moeckel, W. E., and Weston, Kenneth C.: Composition and Thermodynamic Properties of Air in Chemical Equilibrium. NACA TN 4265, 1958.

2. Kemp, Nelson H., Rose, Peter H., and Detra, Ralph W.: Laminar Heat Transfer Around Blunt Bodies in Dissociated Air. Jour. Aero. Sci., vol. 26, no. 7, July 1959, pp. 421-430.

3. Roberts, Leonard: An Approximate Analysis of Unsteady Vaporization Near the Stagnation Point of Blunt Bodies. NASA TN D-41, 1959.

4. Fay, J. A., and Riddell, F. R.: Theory of Stagnation Point Heat Transfer in Dissociated Air. Jour. Aero. Sci., vol. 25, no. 2, Feb. 1958, pp. 73-85, 121.

5. Georgiev, Steven, Hidalgo, Henry, and Adams, Mac C.: On Ablating Heat Shields for Satellite Recovery. Avco Res. Rep. 65, July 1959.

6. Savin, Raymond C., Gloria, Hermilo R., and Dahms, Richard G.: The Determination of Ablative Properties of Materials in Free-Flight Ranges. NASA TN D-1330, 1962.

7. Scala, Sinclaire M.: Sublimation in a Hypersonic Environment. Jour. Aero/Space Sci., vol. 27, no. 1, Jan. 1960, pp. 1-12.

8. Vojvodich, Nick S.: Performance of Ablative Materials in a High-Energy, Partially Dissociated, Frozen Nitrogen Stream. NASA TN D-1205, 1962.

9. Carslaw, H. S., and Jaeger, J. C.: Conduction of Heat in Solids. First ed. Oxford, Clarendon Press, 1947, p. 56.

10. Anon.: Modern Plastics, Encyclopedia Issue, 1959. (Vol. 36, no. 1A, Sept. 1958.) Bristol, Conn., Breskin Publications and Plastics Catalogue Corp., 1958.

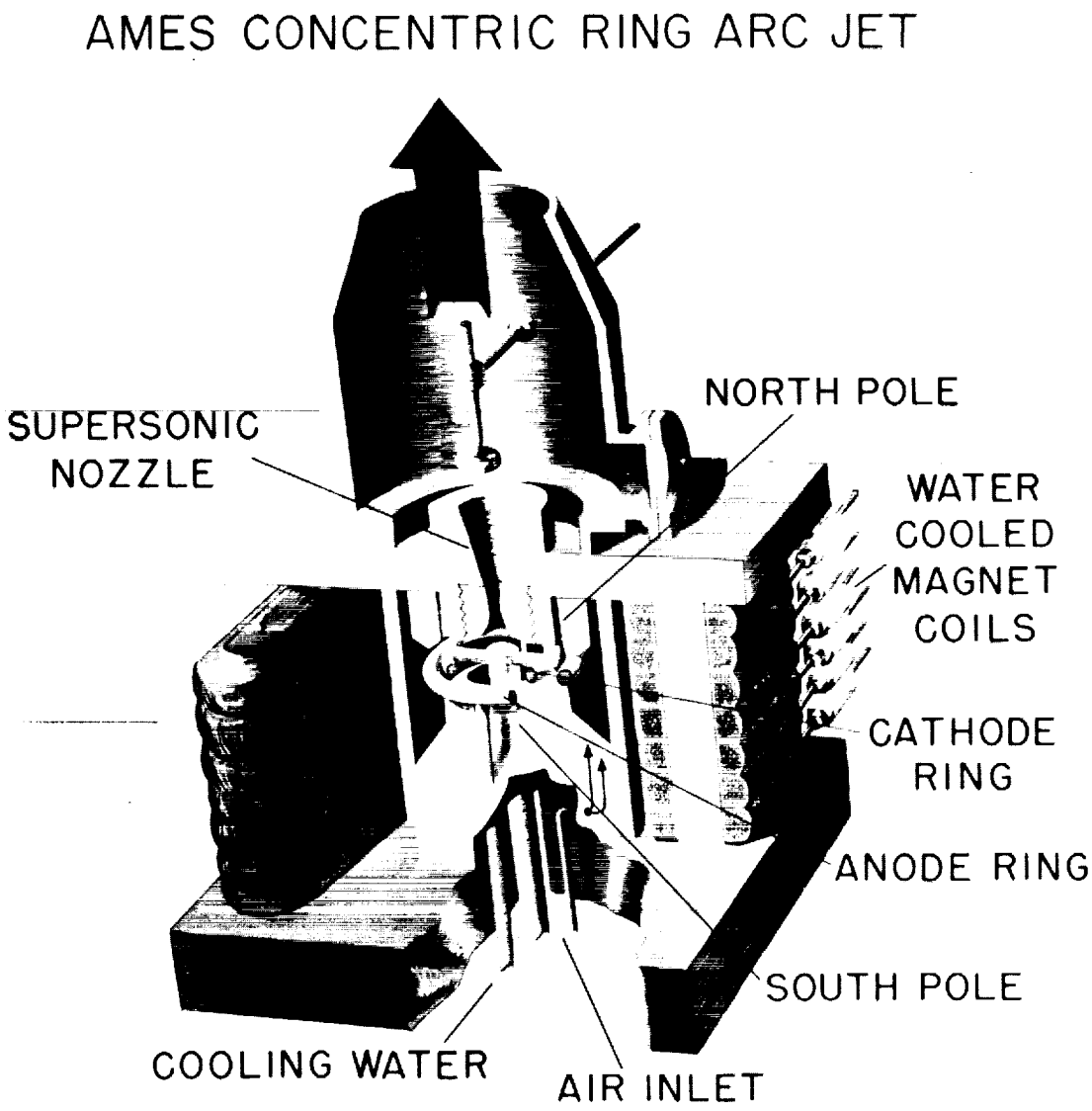

Figure 1.- Arc-jet facility.

A-28321-16

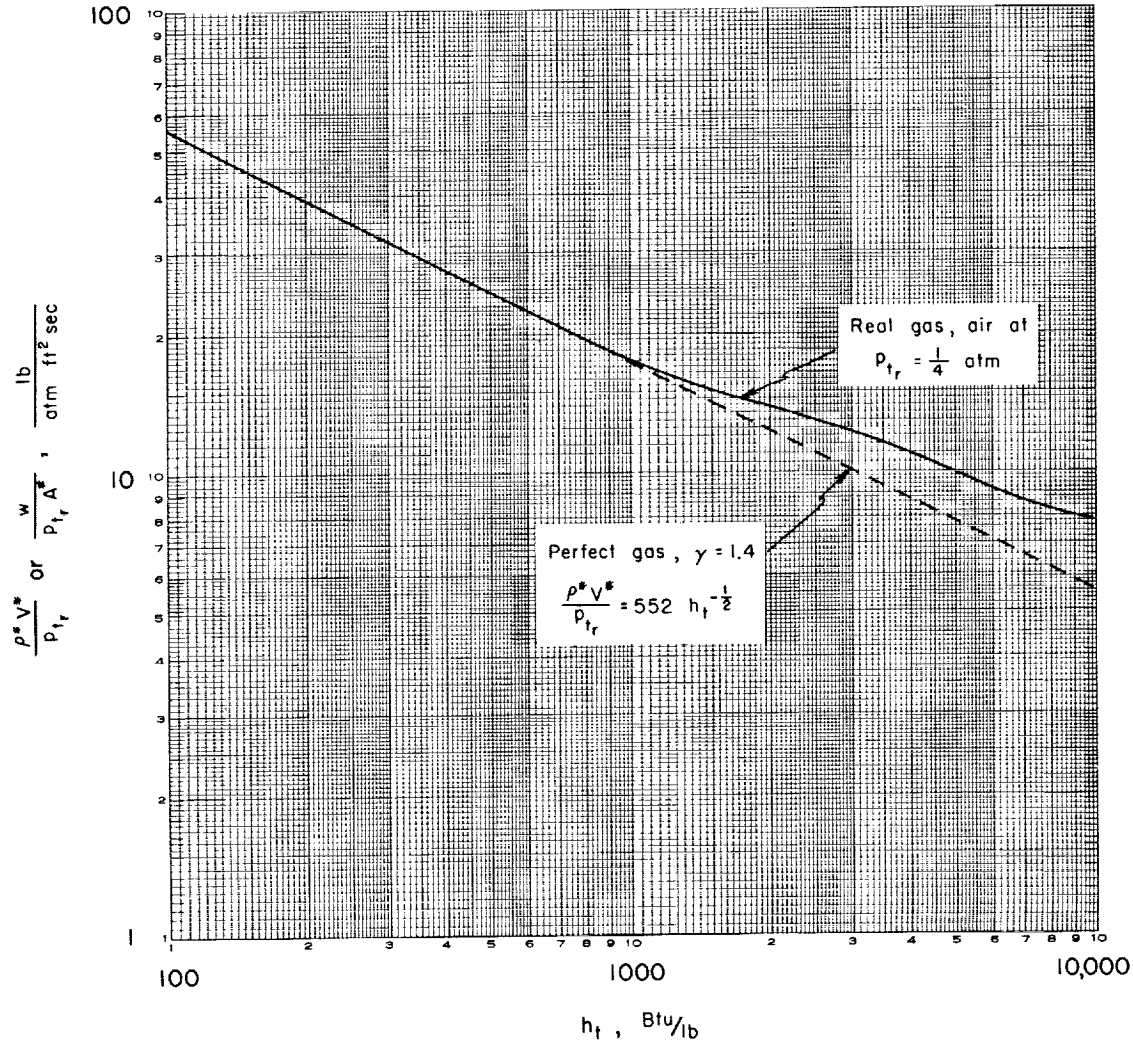

Figure 2.- Variation of $\frac{\rho^* V^*}{p_{t_r}}$ with total enthalpy for equilibrium sonic flow.

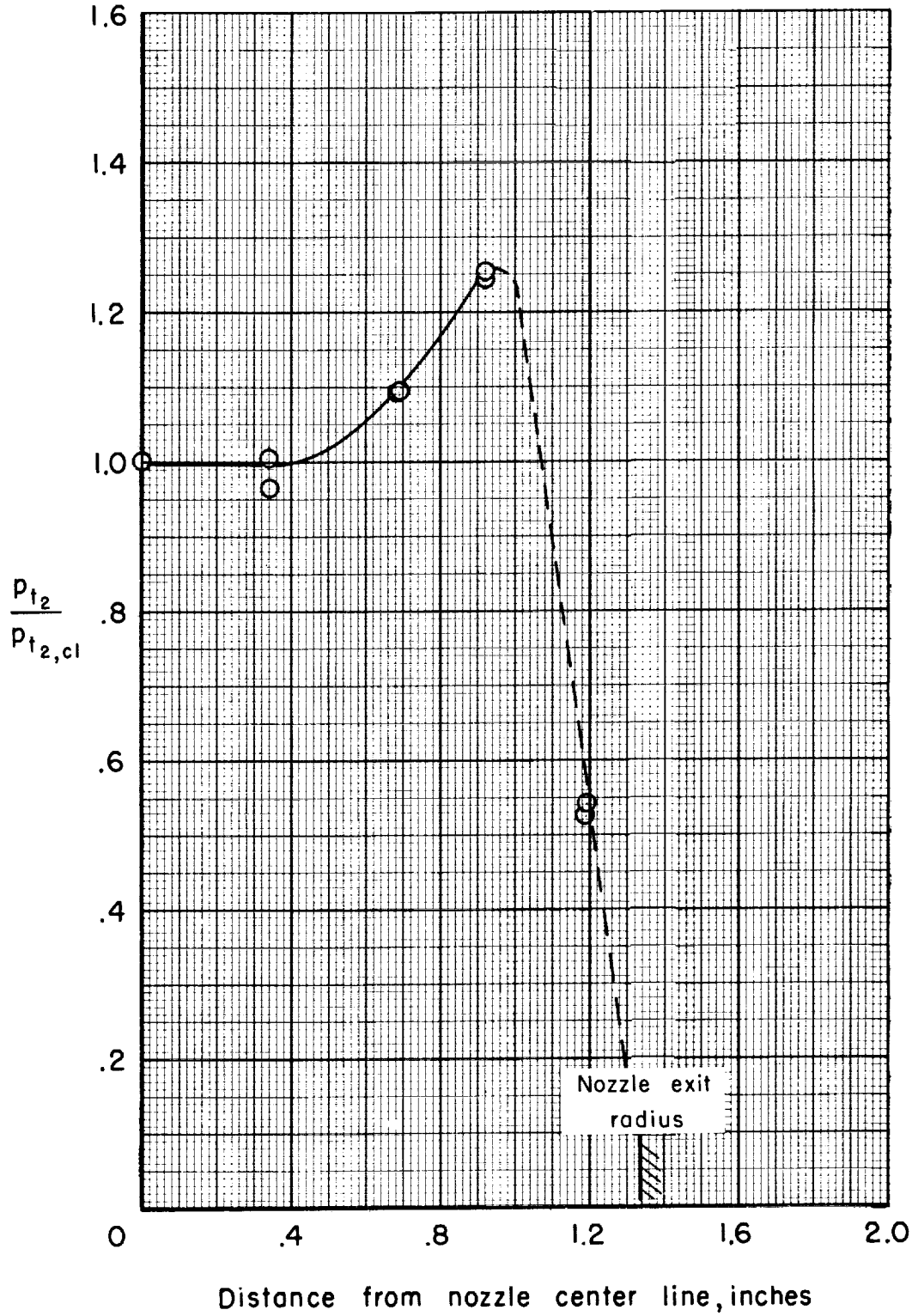

Figure 3.- Radial distribution of total pressure at exit of M = 3.8 nozzle.

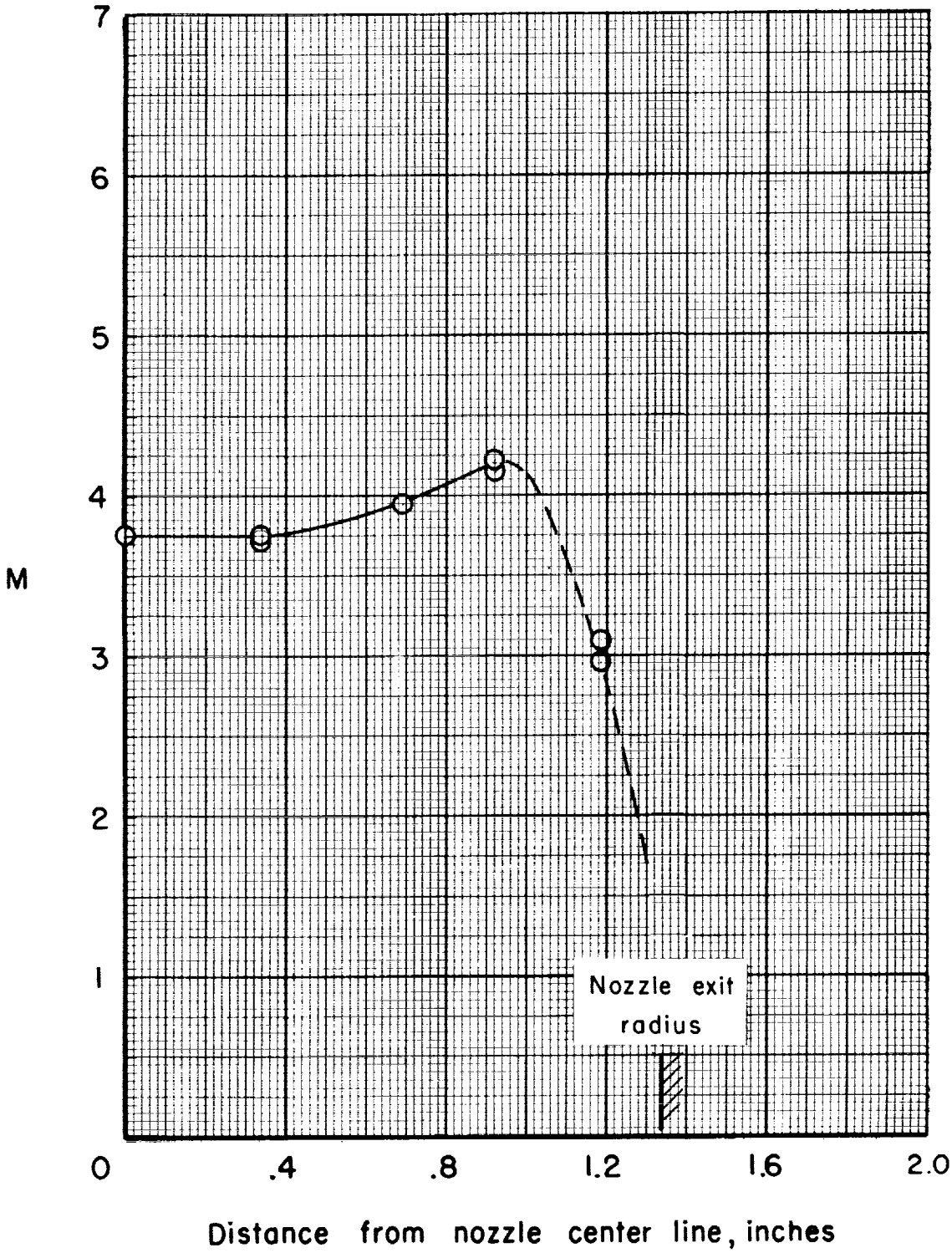

Figure 4.- Radial distribution of Mach number at exit of M = 3.8 nozzle.

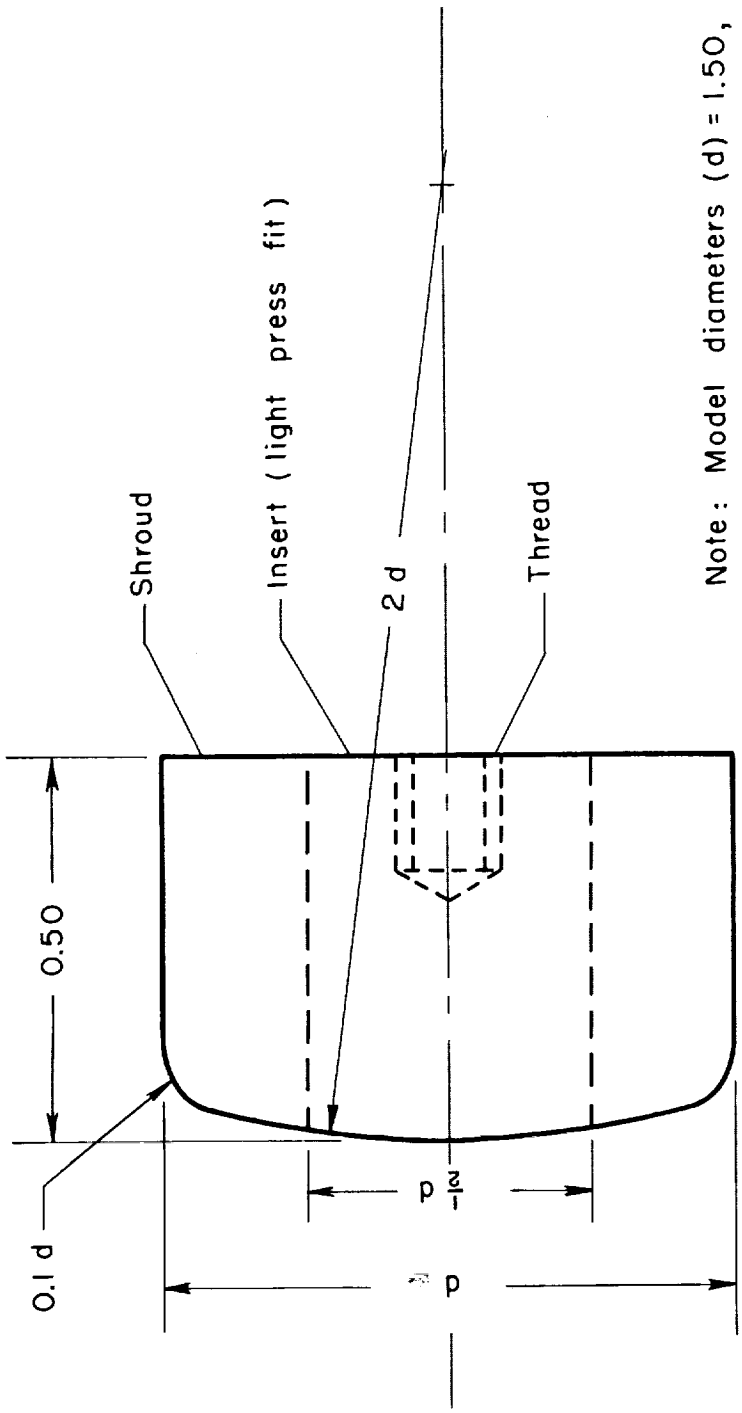

Figure 5.- Sketch of low-heating-rate ablation model.

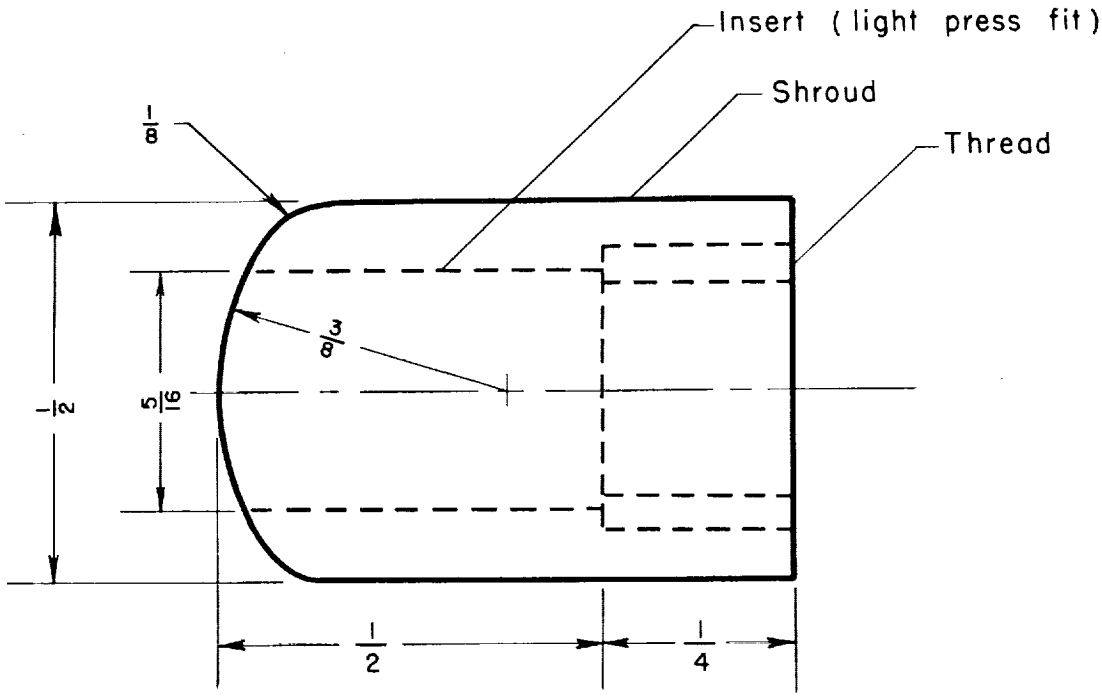

Figure 6.- Sketch of high-heating-rate ablation model.

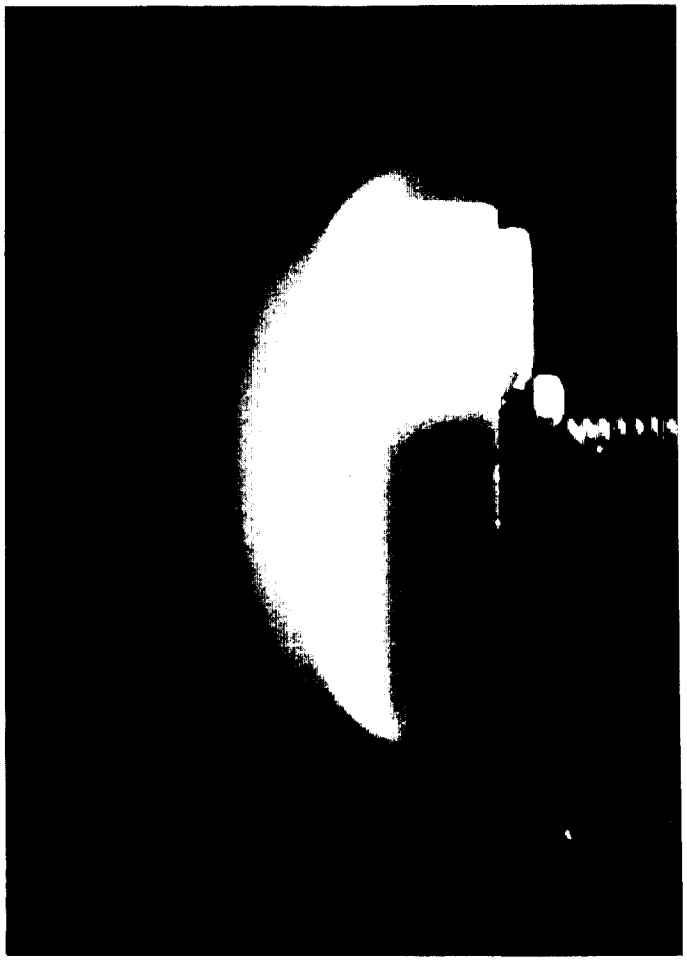

A-27697 (a) Teflon, h_t = 2,190 Btu/lb, $\dot{q}$ = 21.6 Btu/ft^2 sec, model diameter = 1.5 inches.

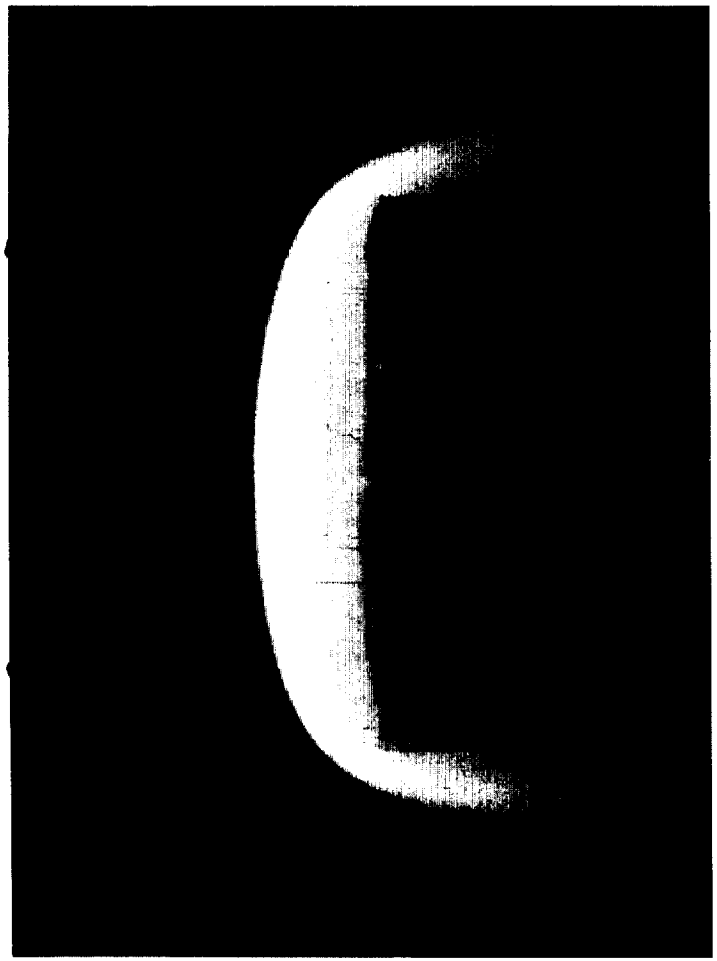

A-27179 (b) Polyethylene, h_t = 2,280 Btu/lb, $\dot{q}$ = 24 Btu/ft^2 sec, model diameter = 1.5 inches.

Figure 7.- Models ablating.

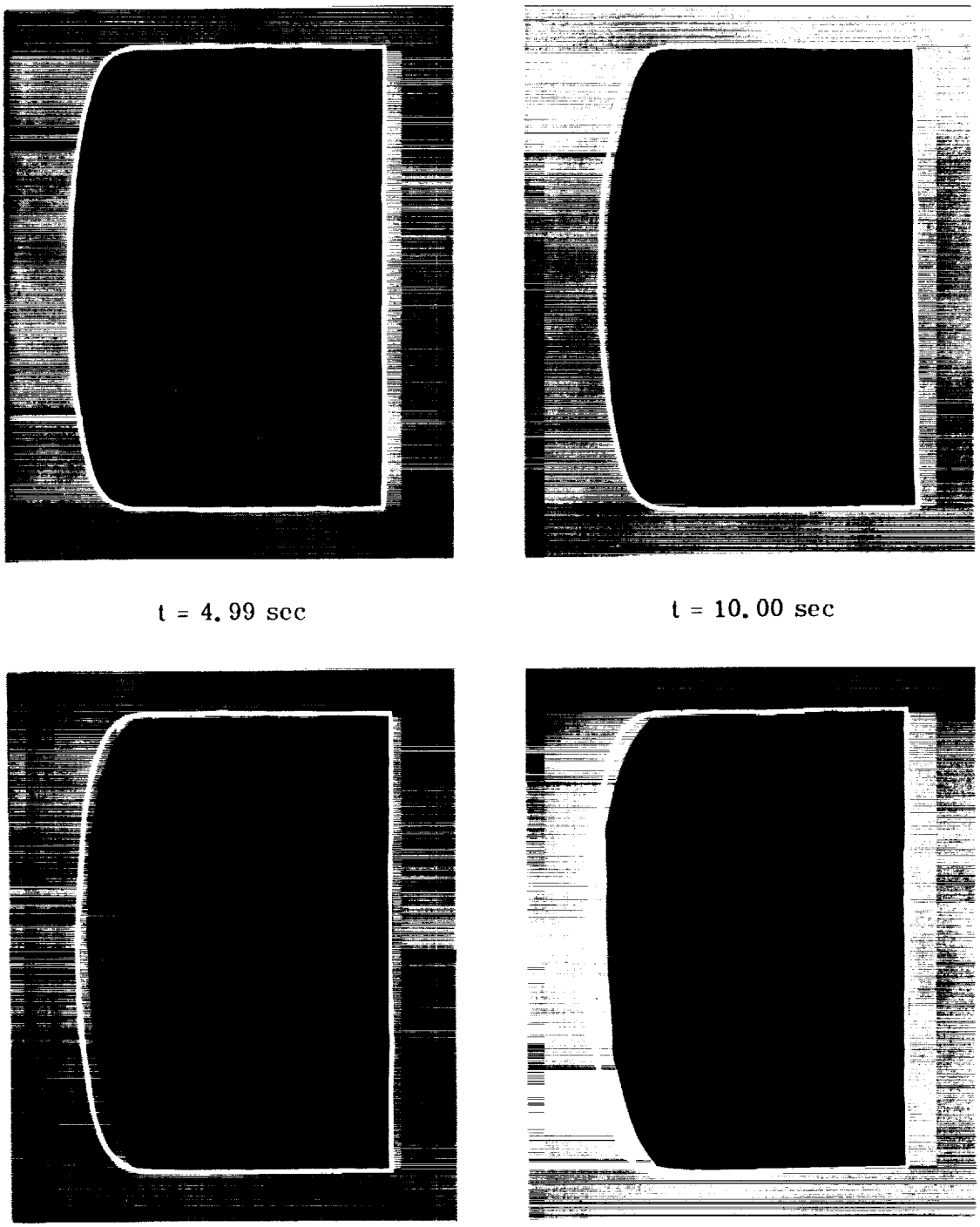

t = 4.99 sec

t = 10.00 sec

t = 15.07 sec

t = 20.21 sec

(a) Teflon, h_t = 2,490 Btu/lb, $\dot{q}$ = 44.7 Btu/ft^2 sec.

Figure 8.- Profiles of 3/4-inch-diameter models before and after ablation.

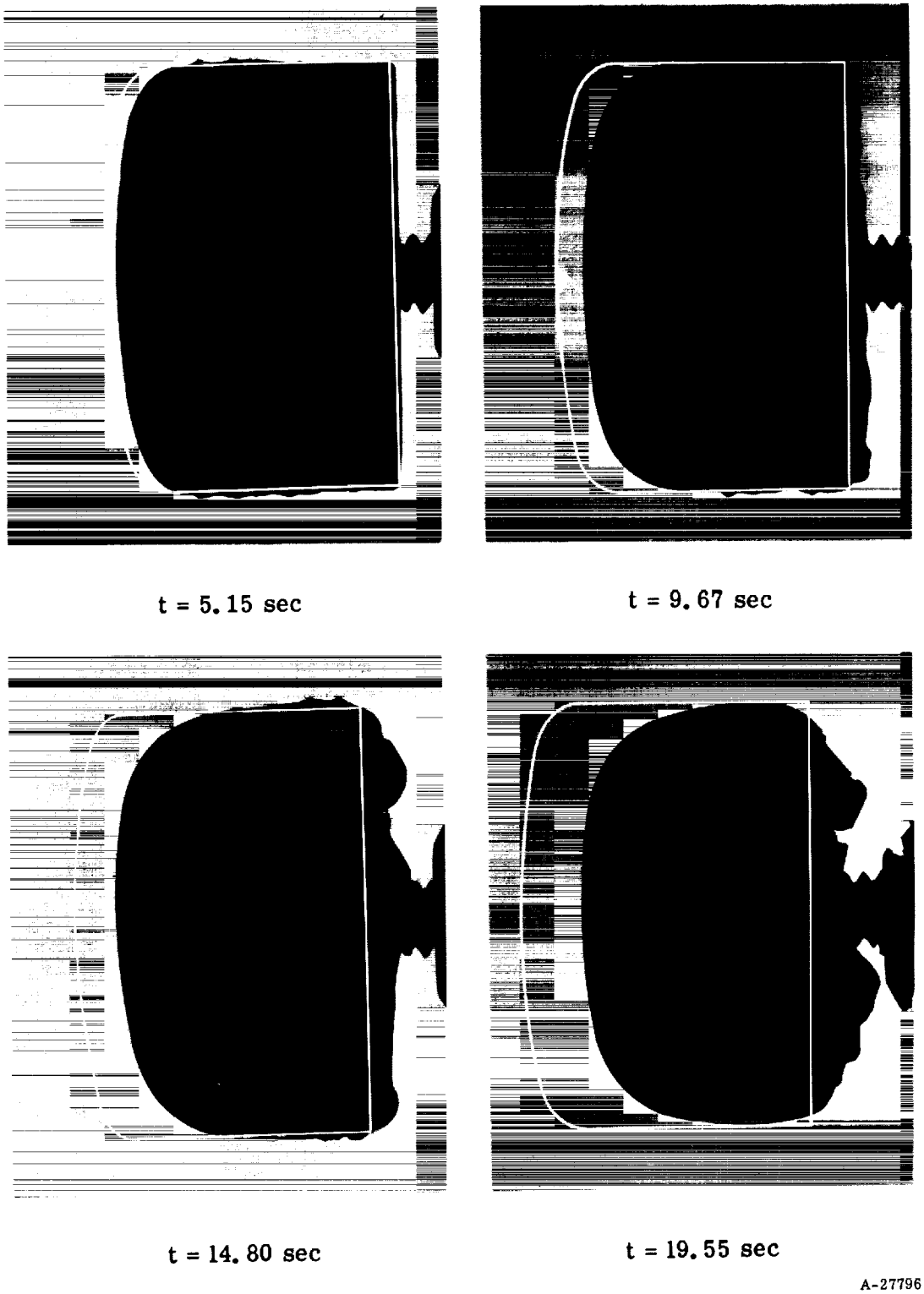

(b) Polyethylene, h_t = 2,320 Btu/lb, $\dot{q}$ = 40.3 Btu/ft^2 sec.

Figure 8.- Concluded.

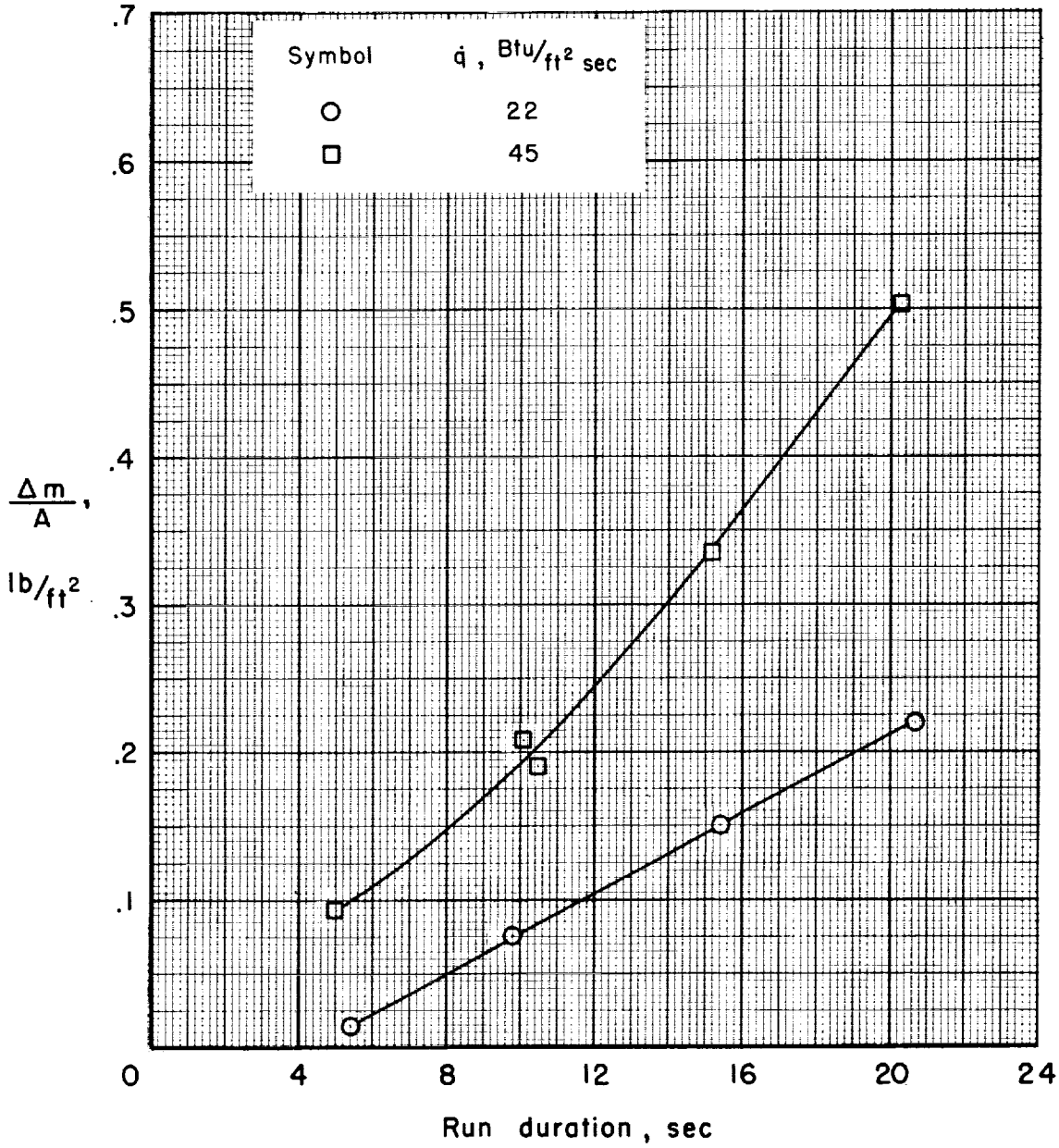

(a) Teflon.

Figure 9.- Mass loss per unit area as a function of run duration.

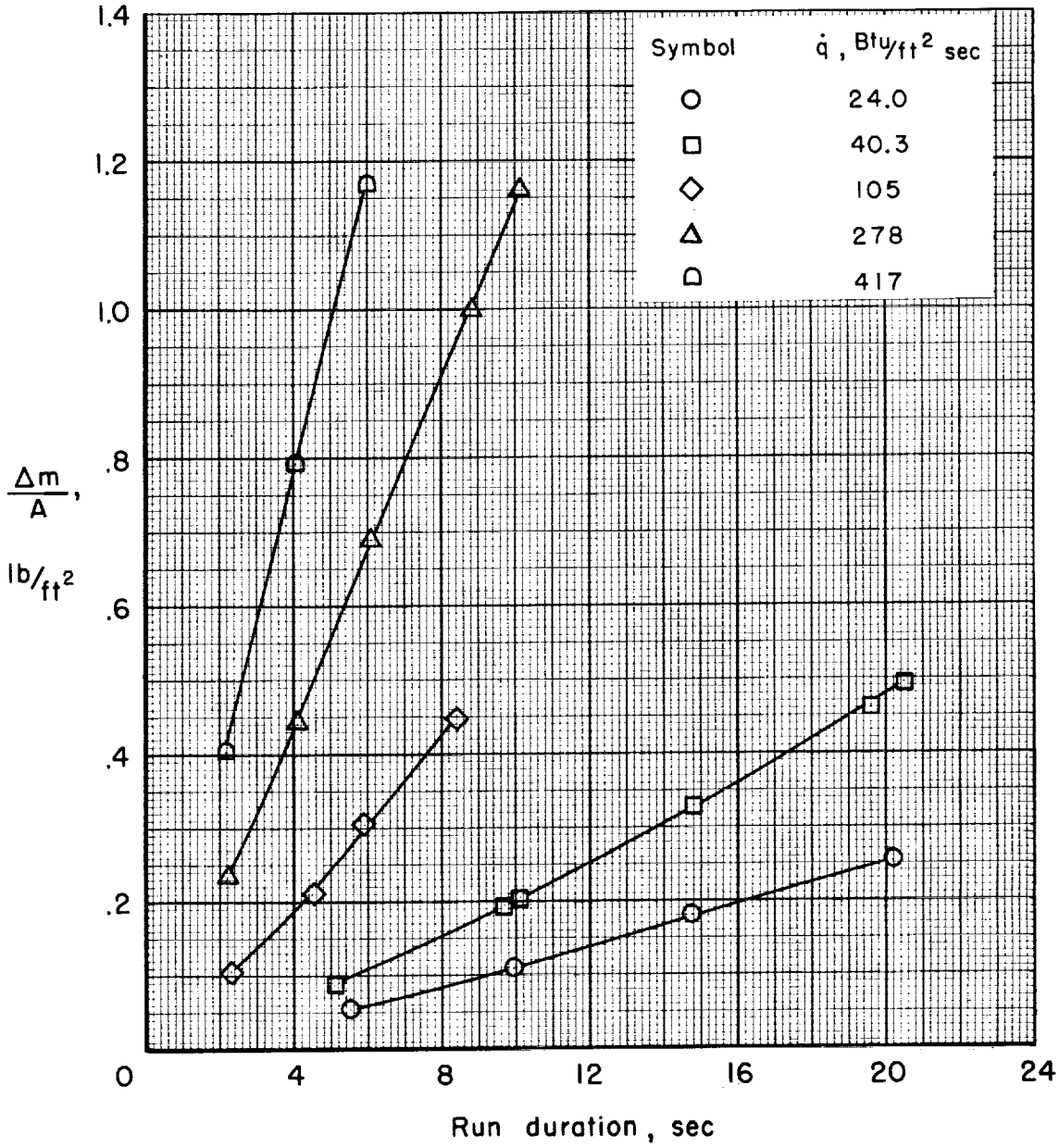

(b) Polyethylene.

Figure 9.- Concluded.

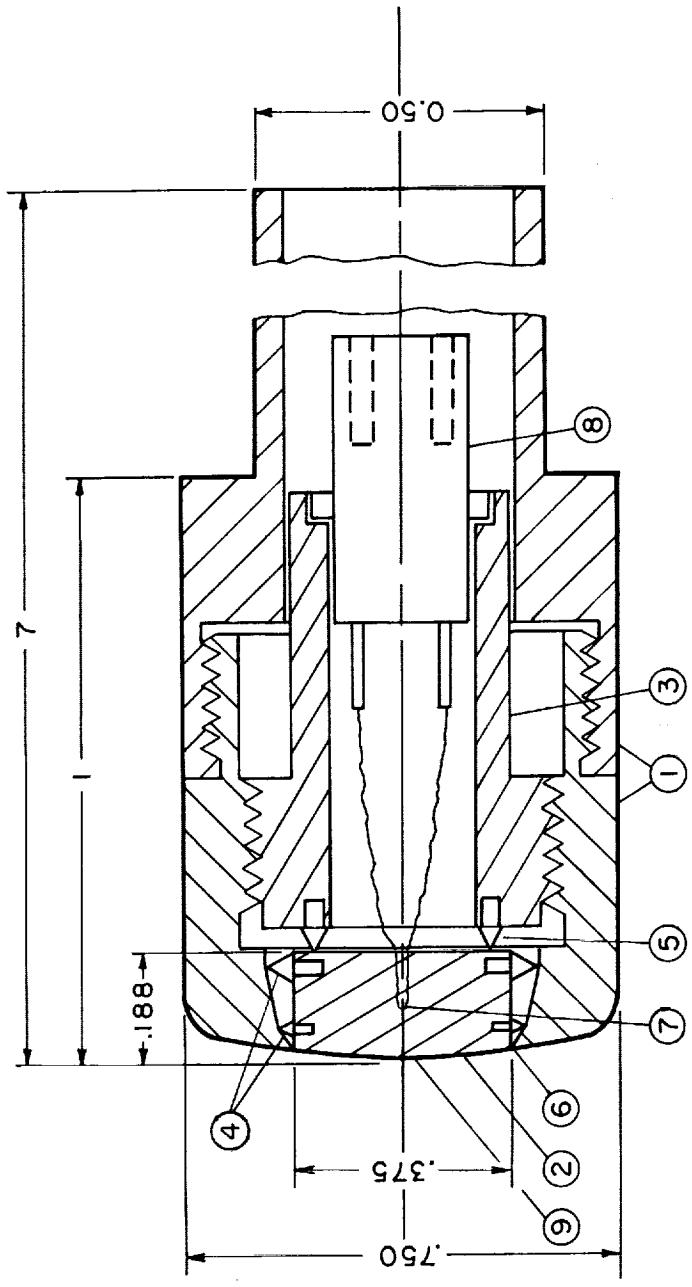

① Shell, stainless steel
② Calorimeter, copper
③ Retainer, bakelite
④ Stainless steel pins, @ 120°
⑤ Bakelite pins, @ 120°
⑥ .002 Gap
⑦ Chromel-alumel thermocouple
⑧ Thermocouple connector
⑨ Radius of curvature = 1.500

All dimensions in inches - only important dimensions shown

Figure 10.- Sketch of 3/4-inch-diameter heat-transfer model.

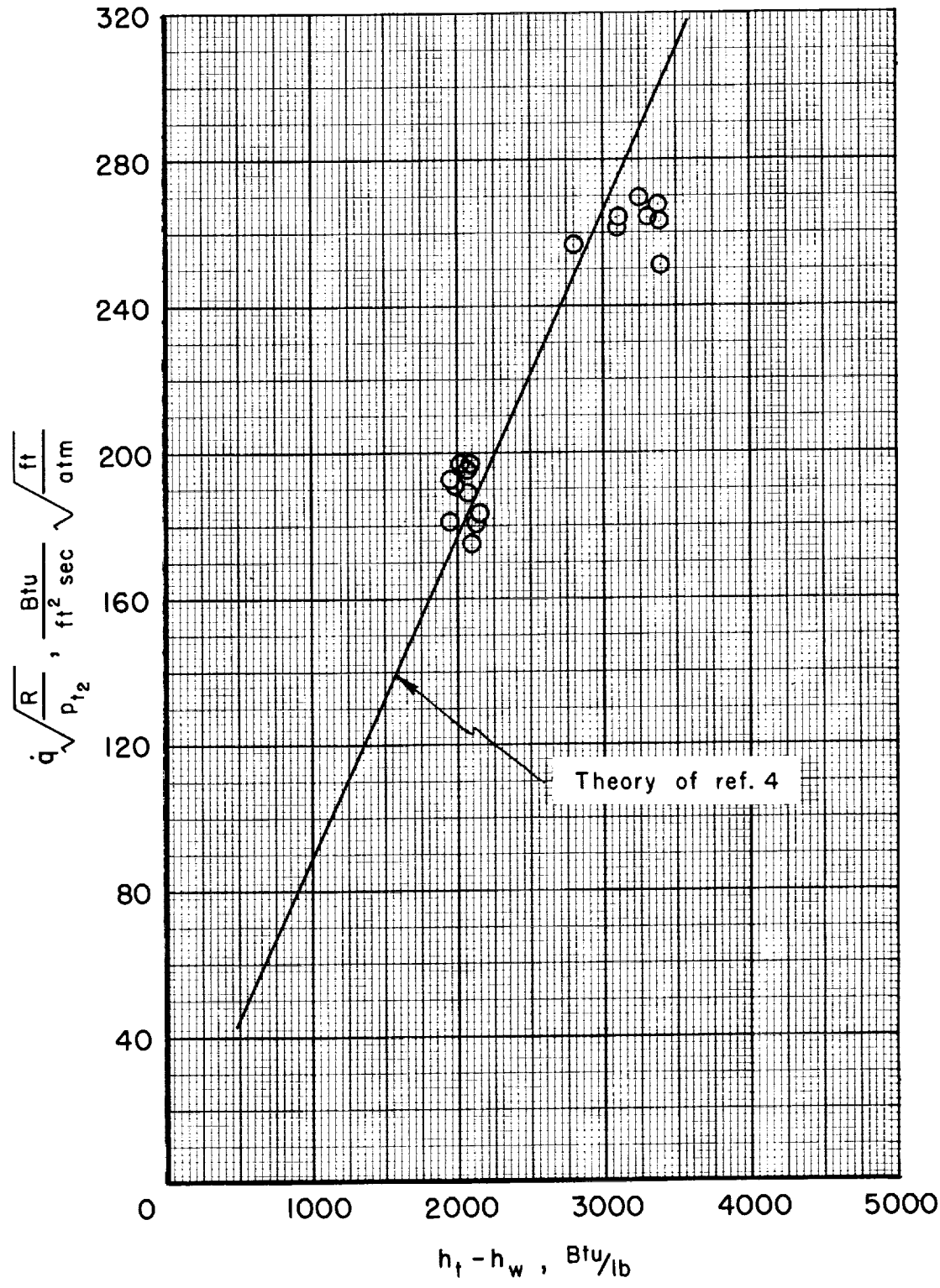

Figure 11.- Representative heat-transfer results.

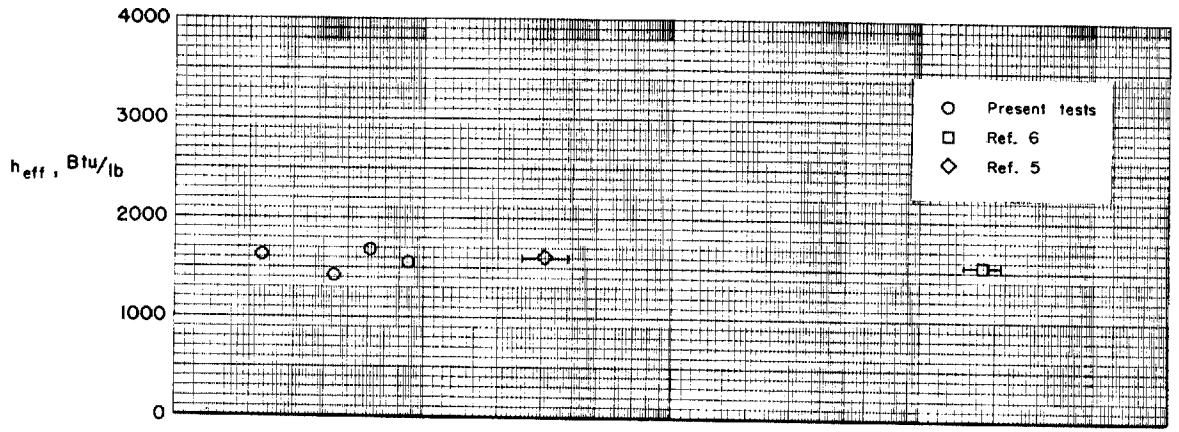

(a) Teflon.

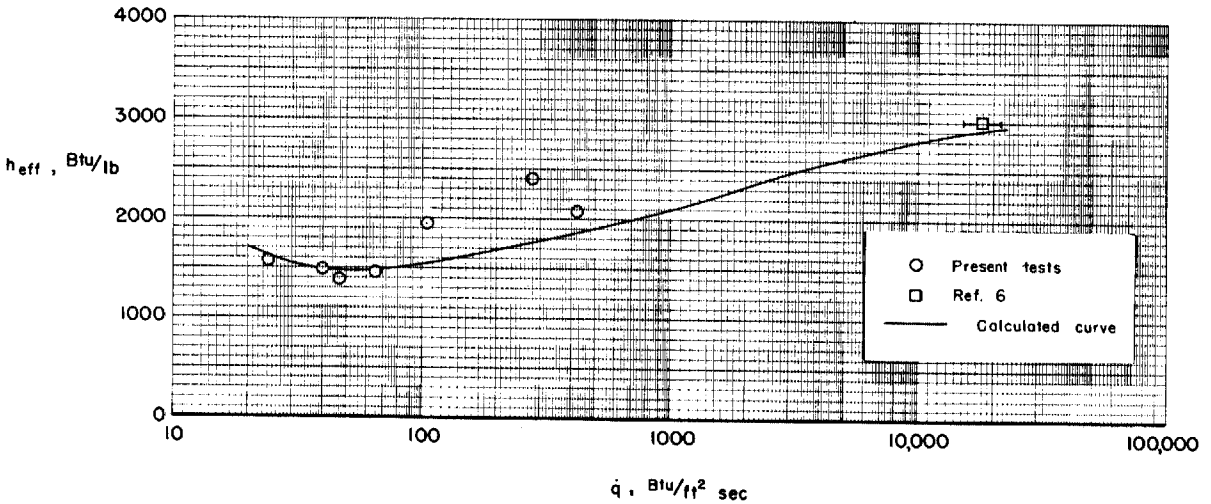

(b) Polyethylene.

Figure 12.- Effective heat of ablation as a function of heating rate for a nominal total enthalpy of 2,500 Btu/lb.

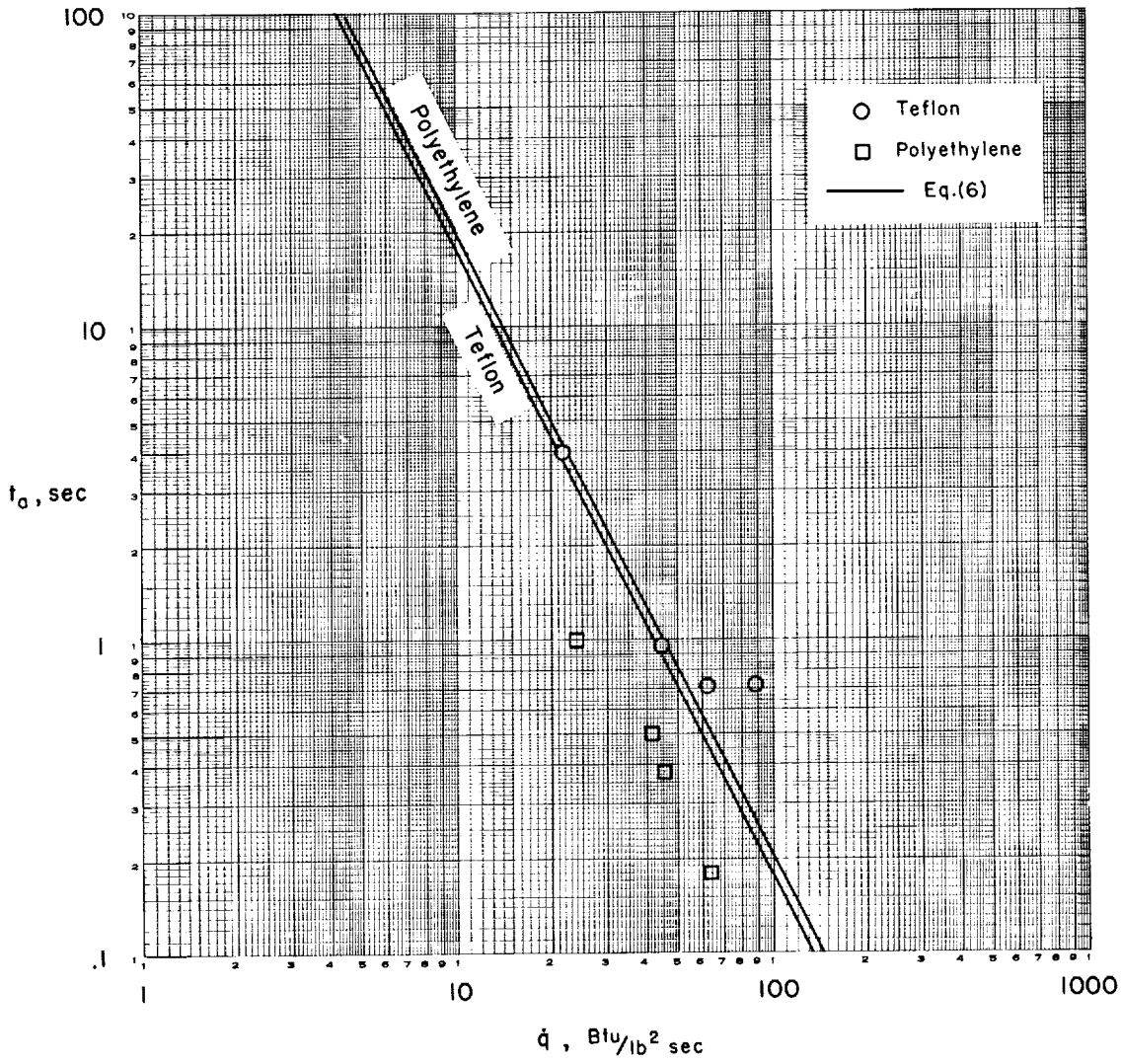

Figure 13.- Time required for the model surface to reach the ablation temperature.

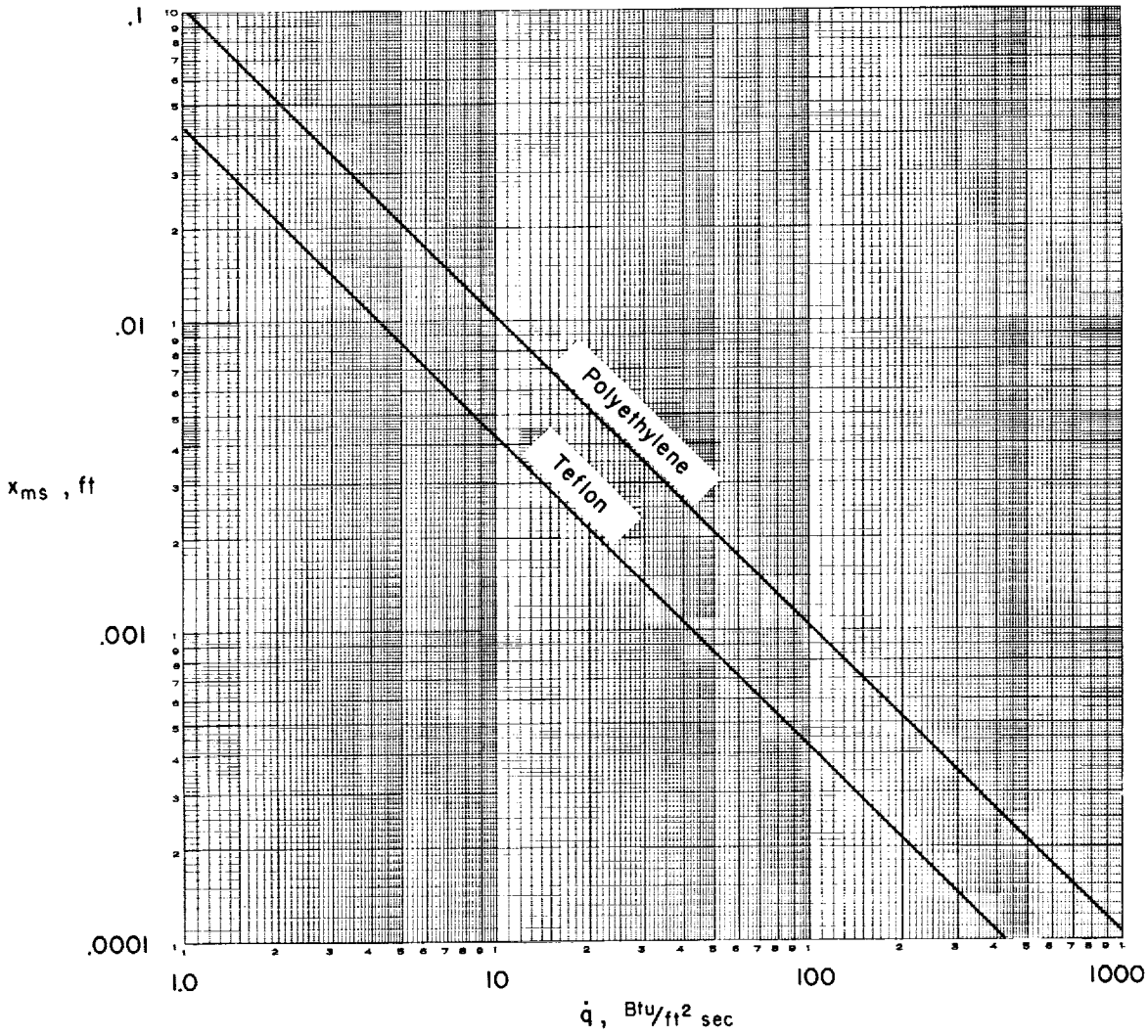

Figure 14.- Depth of penetration of the maximum service temperature into the ablation material at the time ablation begins.

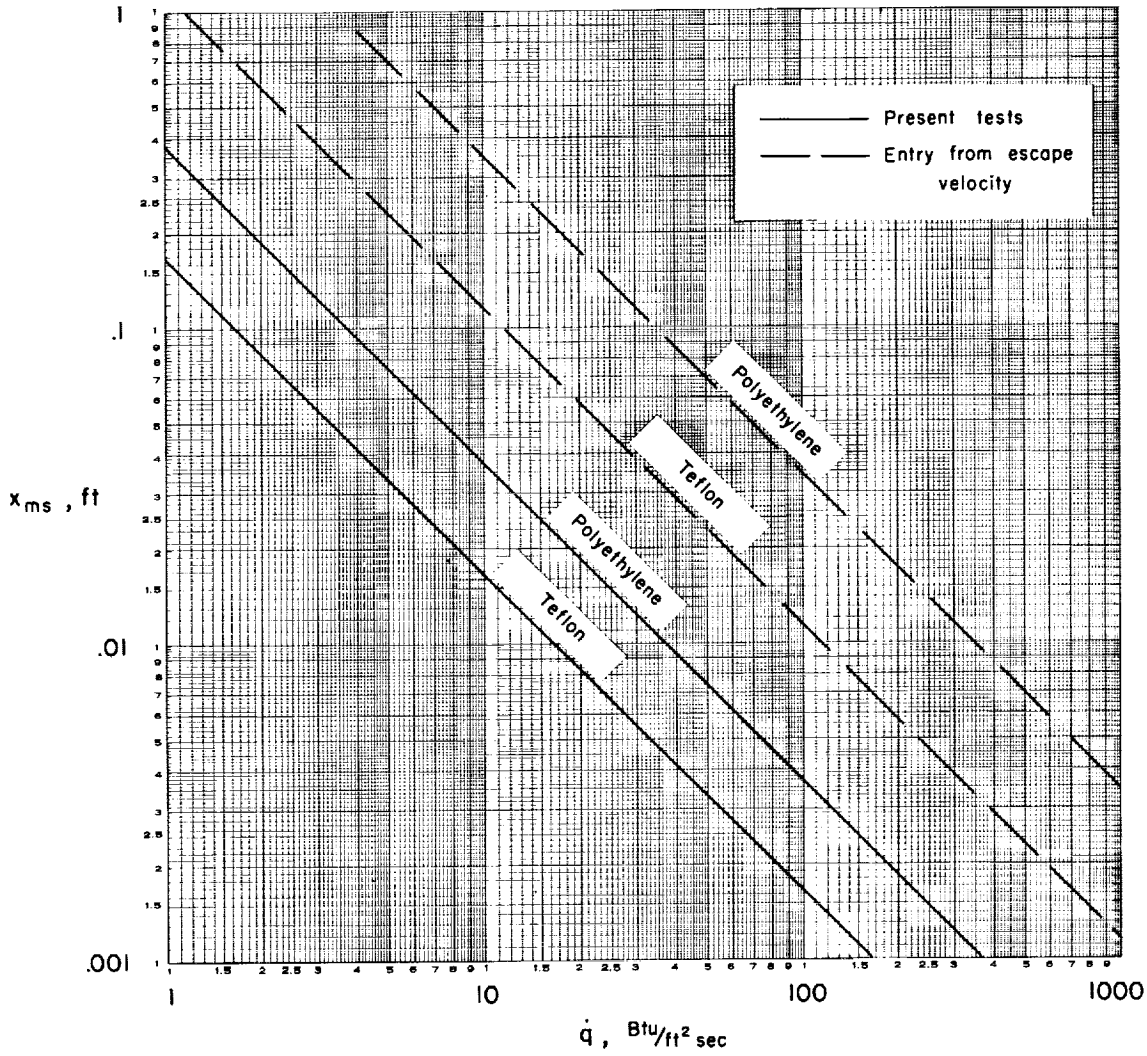

Figure 15.- Depth of penetration of the maximum service temperature into the ablation material for steady-state ablation.

NASA TN D-1332
National Aeronautics and Space Administration.
MEASUREMENTS OF THE EFFECTIVE HEATS OF ABLATION OF TEFLON AND POLYETHYLENE AT CONVECTIVE HEATING RATES FROM 25 TO 420 BTU/FT^2 SEC. Dale L. Compton, Warren Winovich, and Roy M. Wakefield. August 1962. 31p. OTS price, $1.00.
(NASA TECHNICAL NOTE D-1332)

Ablation tests at a nominal total enthalpy of 2,500 Btu/lb showed that the effective heat of ablation for Teflon is independent of heating rate in the range from 25 to 21,000 Btu/ft^2 sec and that the effective heat of ablation for polyethylene at 25 to 420 Btu/ft^2 sec is reduced to 50 to 75 percent of its value at 15,000 to 20,000 Btu/ft^2 sec. Computations are shown for the depth of penetration into these two ablation materials of the maximum temperature for which the materials are structurally useful, for various combinations of heating rate and total enthalpy.

I. Compton, Dale L.
II. Winovich, Warren
III. Wakefield, Roy M.
IV. NASA TN D-1332

(Initial NASA distribution: 14, Chemistry, organic; 25, Materials, engineering.)

NASA

NASA TN D-1332
National Aeronautics and Space Administration.
MEASUREMENTS OF THE EFFECTIVE HEATS OF ABLATION OF TEFLON AND POLYETHYLENE AT CONVECTIVE HEATING RATES FROM 25 TO 420 BTU/FT^2 SEC. Dale L. Compton, Warren Winovich, and Roy M. Wakefield. August 1962. 31p. OTS price, $1.00.
(NASA TECHNICAL NOTE D-1332)

Ablation tests at a nominal total enthalpy of 2,500 Btu/lb showed that the effective heat of ablation for Teflon is independent of heating rate in the range from 25 to 21,000 Btu/ft^2 sec and that the effective heat of ablation for polyethylene at 25 to 420 Btu/ft^2 sec is reduced to 50 to 75 percent of its value at 15,000 to 20,000 Btu/ft^2 sec. Computations are shown for the depth of penetration into these two ablation materials of the maximum temperature for which the materials are structurally useful, for various combinations of heating rate and total enthalpy.

I. Compton, Dale L.
II. Winovich, Warren
III. Wakefield, Roy M.
IV. NASA TN D-1332

(Initial NASA distribution: 14, Chemistry, organic; 25, Materials, engineering.)

NASA

NASA TN D-1332
National Aeronautics and Space Administration.
MEASUREMENTS OF THE EFFECTIVE HEATS OF ABLATION OF TEFLON AND POLYETHYLENE AT CONVECTIVE HEATING RATES FROM 25 TO 420 BTU/FT^2 SEC. Dale L. Compton, Warren Winovich, and Roy M. Wakefield. August 1962. 31p. OTS price, $1.00.
(NASA TECHNICAL NOTE D-1332)

Ablation tests at a nominal total enthalpy of 2,500 Btu/lb showed that the effective heat of ablation for Teflon is independent of heating rate in the range from 25 to 21,000 Btu/ft^2 sec and that the effective heat of ablation for polyethylene at 25 to 420 Btu/ft^2 sec is reduced to 50 to 75 percent of its value at 15,000 to 20,000 Btu/ft^2 sec. Computations are shown for the depth of penetration into these two ablation materials of the maximum temperature for which the materials are structurally useful, for various combinations of heating rate and total enthalpy.

I. Compton, Dale L.
II. Winovich, Warren
III. Wakefield, Roy M.
IV. NASA TN D-1332

(Initial NASA distribution: 14, Chemistry, organic; 25, Materials, engineering.)

NASA

NASA TN D-1332
National Aeronautics and Space Administration.
MEASUREMENTS OF THE EFFECTIVE HEATS OF ABLATION OF TEFLON AND POLYETHYLENE AT CONVECTIVE HEATING RATES FROM 25 TO 420 BTU/FT^2 SEC. Dale L. Compton, Warren Winovich, and Roy M. Wakefield. August 1962. 31p. OTS price, $1.00.
(NASA TECHNICAL NOTE D-1332)

Ablation tests at a nominal total enthalpy of 2,500 Btu/lb showed that the effective heat of ablation for Teflon is independent of heating rate in the range from 25 to 21,000 Btu/ft^2 sec and that the effective heat of ablation for polyethylene at 25 to 420 Btu/ft^2 sec is reduced to 50 to 75 percent of its value at 15,000 to 20,000 Btu/ft^2 sec. Computations are shown for the depth of penetration into these two ablation materials of the maximum temperature for which the materials are structurally useful, for various combinations of heating rate and total enthalpy.

I. Compton, Dale L.
II. Winovich, Warren
III. Wakefield, Roy M.
IV. NASA TN D-1332

(Initial NASA distribution: 14, Chemistry, organic; 25, Materials, engineering.)

NASA

ERRATA

NASA Technical Note D-1332

MEASUREMENTS OF THE EFFECTIVE HEATS OF ABLATION OF TEFLON AND POLYETHYLENE AT CONVECTIVE HEATING RATES FROM 25 TO 420 BTU/FT^2 SEC

By Dale L. Compton, Warren Winovich, and
Roy M. Wakefield

Page 18: Corrected figure 4 on reverse side.

Issue date: 7-6-64

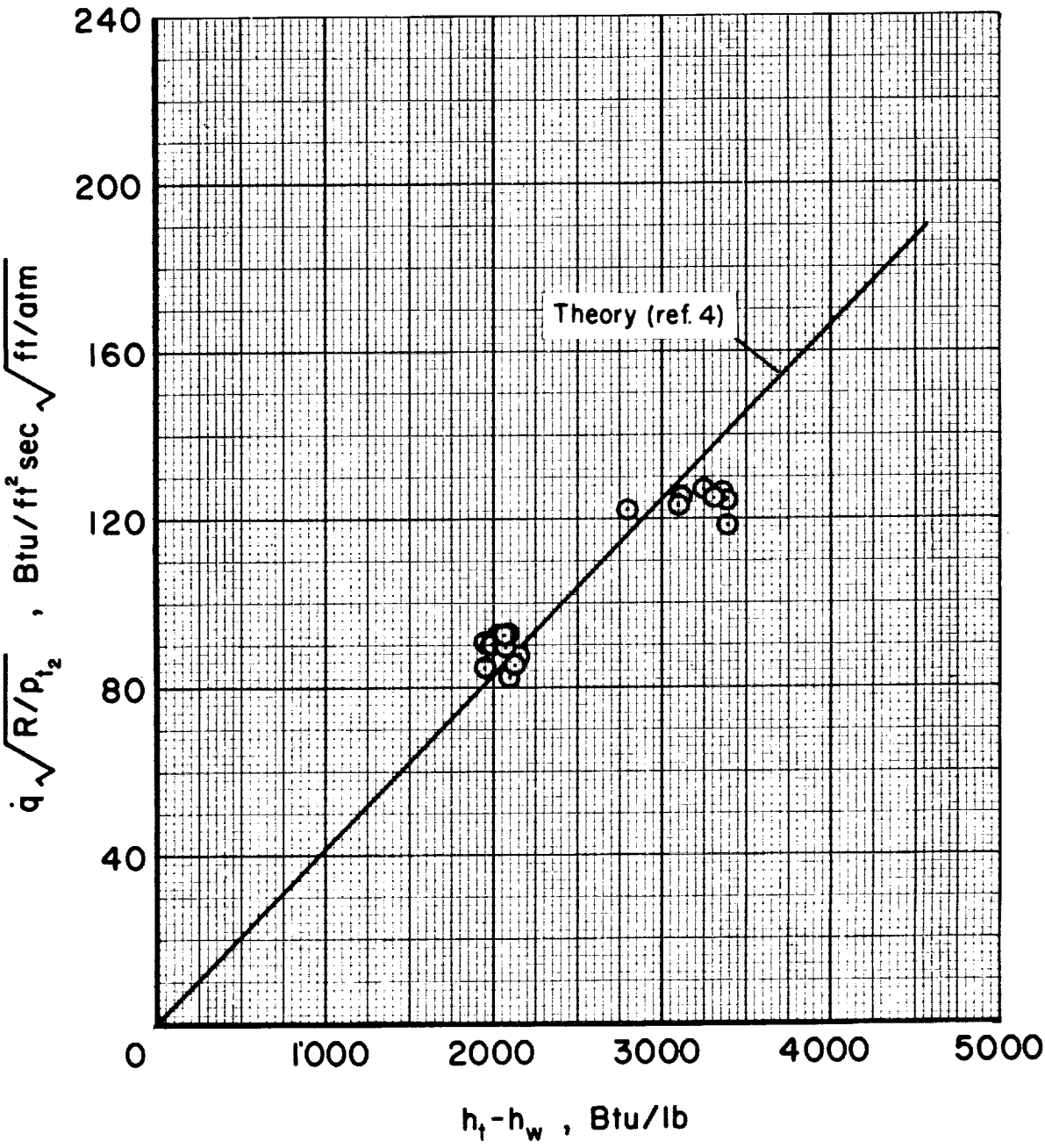

Figure 4.- Radial distribution of Mach number at exit of M = 3.8 nozzle.

NASA-Langley, 1964